

Sodium aluminosilicate synthesised from rice straw as a sorption barrier to protect soil from antimony contamination

A. N. Kholomeydik, A. E. Panasenko & I. V. Kiseleva

To cite this article: A. N. Kholomeydik, A. E. Panasenko & I. V. Kiseleva (05 Dec 2024): Sodium aluminosilicate synthesised from rice straw as a sorption barrier to protect soil from antimony contamination, Chemistry and Ecology, DOI: [10.1080/02757540.2024.2432880](https://doi.org/10.1080/02757540.2024.2432880)

To link to this article: <https://doi.org/10.1080/02757540.2024.2432880>



Published online: 05 Dec 2024.



Submit your article to this journal [↗](#)



View related articles [↗](#)






View Crossmark data [↗](#)

RESEARCH ARTICLE



Sodium aluminosilicate synthesised from rice straw as a sorption barrier to protect soil from antimony contamination

A. N. Kholomeydik ^a, A. E. Panasenko ^a and I. V. Kiseleva ^b

^aInstitute of Chemistry, Far-Eastern Branch, Russian Academy of Sciences Vladivostok, Russia; ^bFederal Scientific Center of the East Asia Terrestrial Biodiversity, Far-Eastern Branch, Russian Academy of Sciences Vladivostok, Russia

ABSTRACT

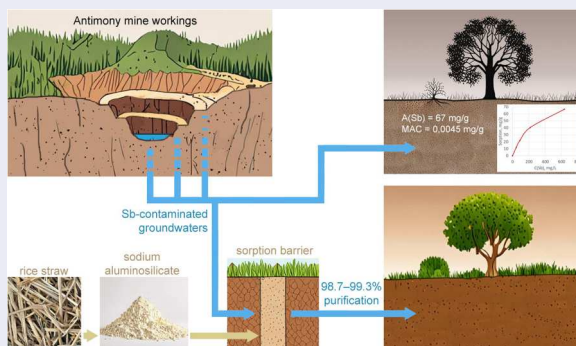
A novel effective sorbent for the extraction of antimony(III) from rice straw has been generated, having a specific surface area of 470 m²/g. The material was subjected to a series of analyses, including scanning electron microscopy, energy dispersive X-ray analysis, X-ray diffraction analysis, and FT-IR spectroscopy. The sorption properties relative to Sb(III) ions were characterised in dynamic conditions in a column experiment. The total dynamic exchange sorption capacity of 113.92 mg/g renders this material suitable for use as a permeable reactive barrier (sorption barrier) with the objective of protecting soils from antimony contamination. To identify the optimal conditions for soil protection, the chemical composition, acid-base properties, and sorption parameters of soils of varying types were characterised. The sorption properties of the soils were determined in static conditions to obtain the sorption isotherm. The maximal sorption capacity was identified for the soil sample with low base saturation and a high organic component content, a finding that was corroborated by DTA analysis. The results of the column experiment with layers of soil and aluminosilicate sorbent indicate the promising use of the new sorbent as a sorption barrier for the effective protection of soils from antimony contamination.

ARTICLE HISTORY

Received 31 July 2024
Final Version Received 19 November 2024

KEYWORDS

Soil; antimony; permeable reactive barrier; sorption barrier; sorbent; aluminosilicate



Introduction

The contamination of environmental waters with metals and metalloids may occur in the vicinity of mineral deposits and mine workings [1]. In particular, acid mine drainage (AMD), which is typified by a low pH and high concentrations of acidic anions and toxic metals, is responsible for the deterioration of the quality of surface streams and groundwater as well as soils [2]. The contamination of regions with antimony, polymetallic, and coal deposits is a significant environmental issue, particularly in the vicinity of the Xikuangshan antimony deposit in China [3,4]. Additionally, antimony is highly concentrated in shooting range soils [5], and landfill leachate also contributes to groundwater pollution with antimony. The high toxicity of antimony(III) makes it imperative to protect the environment from its spread [6].

Various sorption materials are often used for the extraction of metal ions, ranging from simple sorption materials such as plant waste (rice husks, orange peel, coconut coir, etc.) [7–9] to high-tech materials such as the following metal-organic frameworks (MOFs) [10] and covalent organic frameworks (COFs) [11].

A cost-effective approach to the prevention of groundwater contamination or the clean-up of contaminated groundwater involves the application of in-situ permeable reactive barriers (PRBs) or sorption barriers [12,13]. One of the most commonly utilised variants is the PRB with zero-valent iron (ZVI), which is capable of interacting with a range of substances, including antimony. The remediation occurs via reductive processes that are associated with surface corrosion of the iron metal [14]. It is anticipated that Sb^0 will precipitate on the Fe^0 [15]. A study examining the use of iron-containing composite materials in electrokinetic-permeable reactive barriers (EK-PRBs) demonstrated the adsorption capacity relative to Sb(III) to be up to 82.31 mg g^{-1} , a relatively modest figure.

The identification of cost-effective and efficient reactive materials represents a significant challenge in the context of PRBs [16]. Materials that are capable of sorbing antimony typically exhibit a low sorption capacity. Accordingly, the authors [17] indicate that florasil ‘effectively’ can remove Sb(III) from aqueous solutions, while its sorption capacity is approximately 6 mg/g . The natural aluminosilicates kaolinite and nontronite have been observed to exhibit sorption capacity for antimony up to 123 mg/g [18]. Most of the materials studied typically exhibit a sorption capacity for antimony of approximately $100\text{--}250 \text{ mg/g}$, with the exception of the only mixed-oxide mineral birnessite, which has a capacity of 759 mg/g [19]. However, the birnessite mineral is not a common occurrence, and its high cost limits its practical applications.

In order to ensure economic feasibility, composite reactive media derived from waste materials are employed. Including plant and silicate materials have demonstrated high efficiency, with removal rates of $67.3\text{--}99.3\%$ for various metals [16,20].

As previously demonstrated [21], the sodium aluminosilicate derived from rice straw exhibits a maximum sorption capacity for antimony of 596 mg/g under static conditions, which significantly exceeds the capacity of analogous materials. The synthesis of this aluminosilicate simultaneously allows the utilisation of rice straw, which is a highly promising, inexpensive, and renewable raw material.

In order to utilise effective sorption materials as PRBs, two factors must be taken into account. Firstly, in order to optimise the design of a barrier, it is essential to gain an understanding of the dynamic sorption characteristics. This will enable the establishment of the optimal residence time and velocity of groundwater flow.

Secondly, the relevance and efficacy of PRBs is contingent upon the specific type of host soil. It is established that natural soils act as protective barriers against the migration of toxic substances. The natural barrier capacities of soils appear to be a promising method for preventing the spread of pollutants [22]. It is crucial to comprehend the sorption characteristics of the soil in order to make an informed decision regarding the installation of a barrier. Antimony immobilisation in soils is known to depend on both the species composition of the microbiome and the composition of the mineral component, in particular redox-active mineral phases [23].

The objective of the proposed study is to investigate the parameters of dynamic sorption in a column experiment of a novel, environmentally friendly, and cost-effective aluminosilicate, synthesised from rice straw, and also of diverse soil types relative to antimony (III), with the aim of evaluating the efficacy of using a sorption barrier for soil protection.

Materials and methods

The study selected different soil types from various regions of the Russian Far East that were sampled between 2021 and 2022. Soil sections were laid out for sampling and soil samples were collected by genetic horizons using a spade and stiff-bladed knife. The soil samples were taken from four different sections. Section 1 (S1) is located 200 m from the sea, with coordinates N42°49,313' E132°59,702', Haplic Cambisols. Section 2 (S2) is located in an upland area, with coordinates N48°25,993' E134°13,337', Albic Clayic Luvisols. Section 3 (S3) is located in a coastal meadow on a high terrace, with coordinates N49°14,463' E140°19,953', Folic Cambisols (Dystric). Finally, Section 4 (S4) is located on a high coastal terrace with coordinates N45°12,472' E147°50,247', the soil was identified as Ubmbic Cambisols (Humic). Soil names were assigned based on the World Reference Base for Soil Resources [24].

Elemental analysis of the soil was conducted using energy dispersive X-ray fluorescence spectroscopy on a Shimadzu EDX 800 HS spectrometer (Japan). The pH of the water and salt suspensions was measured via potentiometry using a pH meter Mettler Toledo FiveEasy F20 (Switzerland), and the total (hydrolytic) acidity was determined according to Kappen. The organic matter content was estimated by determining the weight loss of the soil upon calcination in a muffle furnace at 900°C (loss on ignition) [25]. The base saturation of soil was calculated using the following formula:

$$V = S / (S + A_{c_{tot}}), \quad (1)$$

where S represents the sum of exchangeable bases and $A_{c_{tot}}$ represents hydrolytic acidity. To ensure the reliability of the results, the analyses were conducted in triplicate to allow for convergence of the data.

The study of the soil absorption capacity for Sb(III) ions was carried out under static conditions from aqueous solutions of SbF_3 with a metal concentration of 50–700 mg/L at a solid/liquid phase ratio (S:L) of 1:1000 at room temperature. To prevent any interaction between the antimony fluoride and glassware, we used PET or polyethylene flasks. We did not adjust the pH of the solutions during the experiment.

We determined the concentration of antimony ions in the solution using atomic absorption spectrometry on an AA-770 spectrophotometer (Nippon Jarrell Ash, Japan) in an acetylene-air flame. For more precise determination, we carried out bromatometric titration.

The sorption capacity of the soils (A , mg/g) was calculated using the following formula:

$$A = (C_i - C_{eq}) \cdot V \cdot 1000/m, \quad (2)$$

where C_i and C_{eq} are the initial and equilibrium concentrations of antimony (mg/mL), V is the volume of the solution (mL), and m is the weight of the sample (g).

Thermal analysis was performed using a MOM Q-1000 derivatograph with a heating rate of 5 K/min. Aluminum oxide calcined at 1000°C was used as a reference sample. The ignition losses were determined after the samples were calcined at 1000 °C for one hour.

Sodium aluminosilicate was synthesised from rice straw using the following method: the straw was treated with 1 M NaOH solution (ratio S:L = 1:13) at 90°C for 1 h. The resulting hydrolysate was separated by filtration from the solid cellulose residue. A dilute aqueous solution of aluminum sulfate was added to the hydrolysate, and the pH of the solution was adjusted to 7. The resulting precipitate was decanted, washed, and dried at 105°C, as described in [26].

The sorption properties of sodium aluminosilicate under dynamic conditions were determined by passing a model solution of SbF_3 through a fixed layer of sorbent. The sorbent fraction had a particle size of 1 mm, and the column inner diameter was 0.5 cm. The ratio of column diameter to height (d:h) was varied in the range of 1:3–1:8. The model solution had an Sb(III) concentration of 50 mg/L and was permeated using a peristaltic pump at a flow rate of 1.5 mL/min. The eluate was collected in 25 mL portions, and the residual Sb content in the solution was determined.

The dynamic exchange sorption capacity (DEC) and total exchange sorption capacity (TDEC) were then calculated using the following equations:

$$DEC = \frac{C_i - C_b}{m} \times V_b, \quad (3)$$

$$TDEC = \frac{\sum (C_i - C_n) \times V_n}{m}, \quad (4)$$

where C_i is the initial concentration of Sb(III) in the model solution in mg/L, C_b is the concentration of Sb(III) at the break point in mg/L, m is the mass of dry sorbent in grams, V_b is the volume of solution before the break point in liters, C_n is the concentration of Sb(III) in each n^{th} portion of the output solution (mg/L), and V_n is the volume of the n^{th} portion of the output solution (L). The antimony break point was determined as the point at which the efficiency of Sb(III) extraction under dynamic conditions decreased to less than 95%.

Results and discussion

The initial stage of the research involved studying the the sorption and barrier properties of, sodium aluminosilicate, derived from the alkaline hydrolysate of rice straw [21]. The sample was analysed for its elemental composition. The material is composed of SiO_2 (48.9%), Al_2O_3 (38.1%), and Na_2O (12.9%), which is approximately consistent with the gross formula $Na_2Si_4Al_4O_{15}$. It is X-ray amorphous, as indicated by a blurred maximum in the X-ray diffraction pattern in the 27° region (Figure 1(a)). The IR spectrum shows absorption bands at 1014 cm^{-1} (ν_{as} Si–O) and 700 cm^{-1} (Al–O–Si), which are specific to

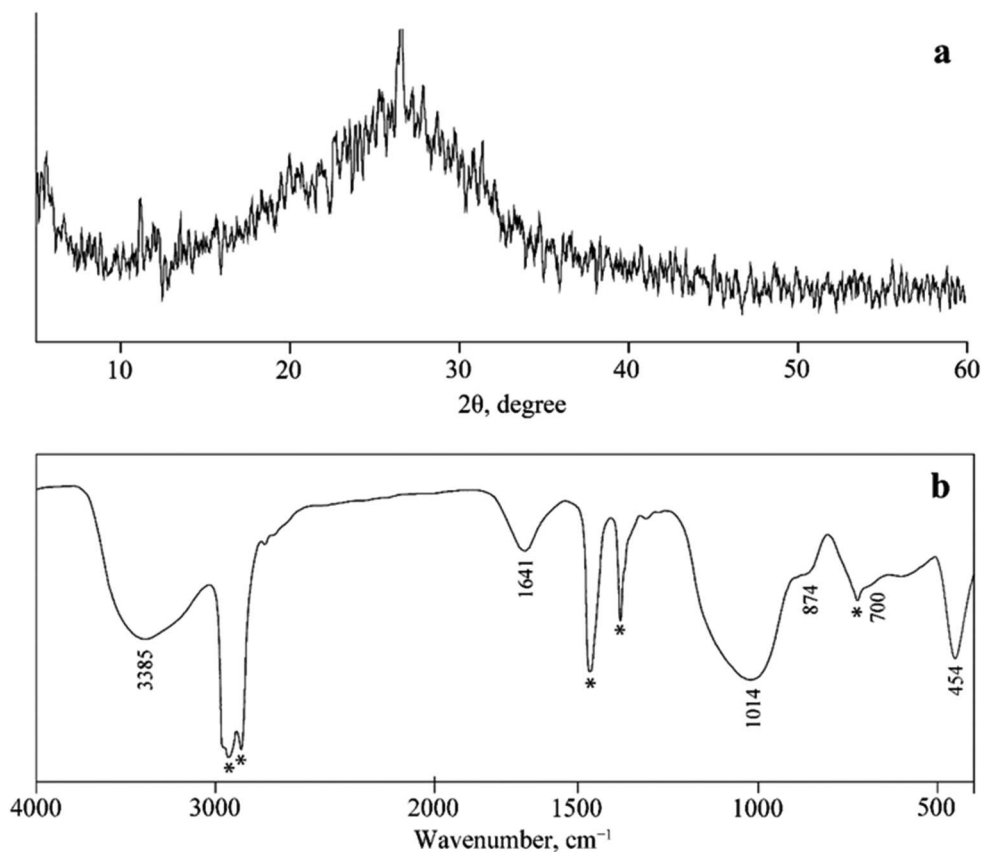


Figure 1. X-ray diffraction pattern (a) and FTIR spectrum (b) of the sodium aluminosilicate synthesised from rice straw and investigated as a sorption barrier.

aluminosilicates (Figure 1(b)). The morphology of the material is disordered, with primary particles smaller than $0.5\ \mu\text{m}$ aggregating into porous agglomerates of a few tens of μm (Figure 2). The specific surface area is $470\ \text{m}^2/\text{g}$.

As demonstrated previously [21], the maximum sorption capacity of sodium aluminosilicate derived from rice straw for antimony under static conditions is $596\ \text{mg/g}$, with a recovery rate of approximately 76%. This capacity significantly exceeds that of commercial analogs, which typically exhibit a sorption capacity of approximately $100\text{--}250\ \text{mg/g}$, except for the only mixed-oxide mineral birnessite, which has a capacity of $759\ \text{mg/g}$ [19]. An additional benefit of this material is that it is synthesised from renewable plant-based resources.

It is established that the sorption mechanism of antimony(III) on biogenic aluminosilicates, resulting from an inhomogeneous surface structure, is a complex process that encompasses chemical interaction [27], cation exchange, and hydrolysis [28].

The study evaluated the absorption capacity of sodium aluminosilicate in dynamic mode at different layer heights. The results are presented in Table 1 and Figure 3. The data show a nonlinear increase in the dynamic exchange capacity with increasing sorbent layer height. Specifically, increasing the sorbent layer by 2.6 times resulted in a

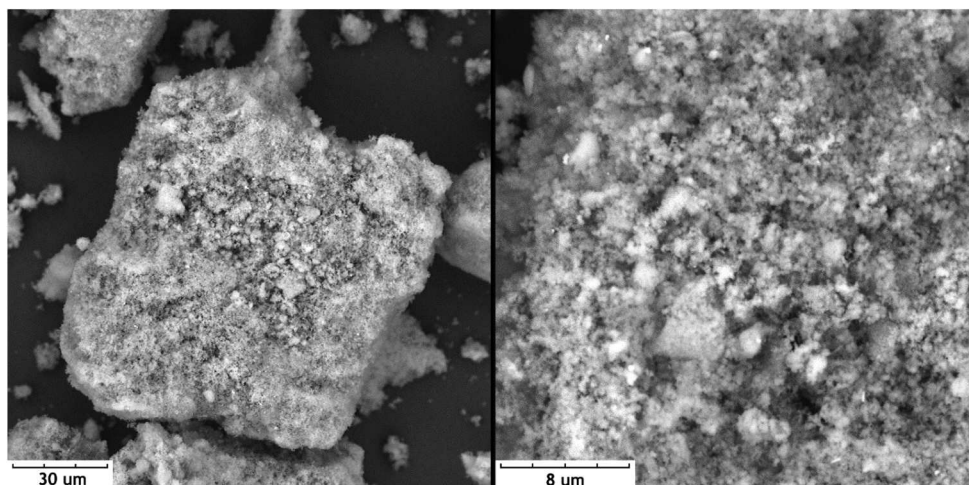


Figure 2. SEM image of the synthesised sodium aluminosilicate.

Table 1. Dynamic and total exchange sorption capacity of biogenic sodium aluminosilicate with respect to Sb(III) ions.

No	d: h	DEC, mg/g	TDEC, mg/g
1	1: 3	7.71	90.25
2	1: 6	40.92	81.26
3	1: 8	59.96	113.92

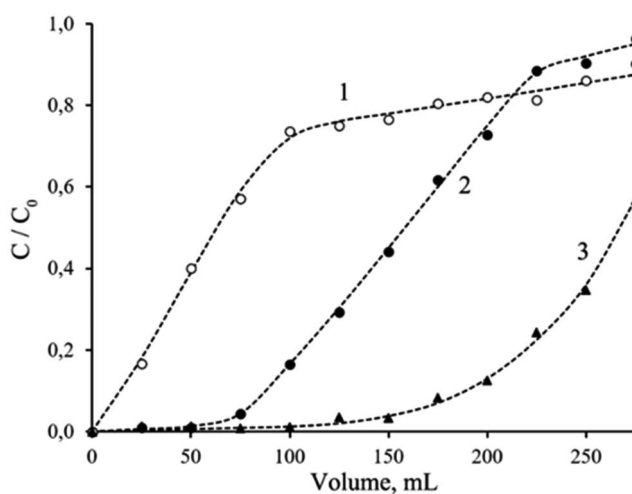


Figure 3. Output curves of antimony(III) ions sorption under dynamic conditions at different sodium aluminosilicate layer heights (d:h): 1–1:3; 2–1:6; 3–1:8.

7.8-fold increase in the specific capacity per unit mass. The total exchange capacity also increased, although insignificantly. When the ratio d:h is equal to 1:8, the degree of purification of the antimony solution at the initial site is within the range of 98.7%–99.3%.

As natural soils also possess sorption barrier capacity and can impede the dissemination of pollutants [22], the second stage of the research sought to examine the sorption capacity of soils in relation to antimony under static conditions. Table 2 presents the elemental composition of the soils under investigation, calculated for the oxides, while Table 3 presents their physicochemical properties.

The maximum sorption capacity of soil for antimony(III) ions varies depending on the soil type and composition, as shown in Figure 4 and Table 3. The sorption properties are related to soil organic matter [29], resulting in a positive correlation between the sorption capacity and ignition loss and a negative correlation between the sorption capacity and SiO₂ content. In addition to the organic matter content, the soil cation exchange properties also significantly influence the soil sorption capacity. The maximum sorption capacity (A_{\max}) is positively correlated with hydrolytic acidity and negatively correlated with soil base saturation (V). For instance, soil S2(0–10) has a high organic matter content and degree of base saturation but a low sorption capacity.

The hydrolytic acidity value indicates the amount of exchangeable hydrogen and aluminum ions that are displaced from the soil absorption complex when the soil interacts with the hydrolytically alkaline salt CH₃COONa. The soil base saturation is the percentage of exchangeable bases (Na⁺, K⁺, Mg²⁺, Ca²⁺ cations) relative to the total amount of exchangeable cations (including hydrogen H⁺ and aluminum Al³⁺) in the soil absorption complex. The correlation between A_{\max} and V confirms that sorption occurs mainly through the exchange of hydrogen and aluminum ions for antimony ions rather than exchangeable bases (Na⁺, K⁺, Mg²⁺, Ca²⁺).

Figure 1 shows that soil sample S3(0–7) has the highest absorption capacity for antimony ions, which is attributed to the high content of organic component in this soil and the low base saturation. The content of organic component in the soil can be

Table 2. Composition of the investigated soils, wt. %.

Section (depth, cm)	SiO ₂	Al ₂ O ₃	Fe ₂ O ₃	K ₂ O	Na ₂ O	CaO	MgO	H ₂ O	SOC	Ignition losses, %
S1 (0–17)	48.8	19.0	8.87	5.71	2.81	1.44	0.40	1.78	4.05	9.90
S1 (17–33)	49.4	25.0	7.57	5.09	2.40	1.01	0.39	0.83	1.65	7.27
S2 (0–10)	44.5	13.5	7.89	3.95	1.61	1.38	0.42	3.80	8.2	21.1
S2 (15–45)	56.8	16.7	10.8	5.82	2.71	0.69	0.38	0.98	1.44	3.70
S3 (0–7)	18.1	8.67	6.21	1.32	0.61	1.0	0.33	6.30	21.4	55.7
S3 (7–27)	33.7	16.8	7.91	2.30	0.92	0.34	0.29	5.71	14.5	30.0
S4 (0–20)	43.3	11.7	11.2	1.3	2.01	2.06	0.36	3.85	8.42	22.8

Table 3. Physicochemical properties of the studied soils: pH of the extracts, hydrolytic acidity (Ac_{tot}), base saturation (V), and maximum sorption capacity toward antimony (A_{\max}).

Section (depth, cm)	pH (H ₂ O)	pH (KCl)	Ac_{tot} (cmol(equiv)/kg)	V, %	A_{\max} (Sb), mg/g
S1(0–17)	6.0	4.9	6.81	92.3	20.89
S1(17–33)	5.8	4.8	4.72	90.6	14.23
S2 (0–10)	5.7	4.7	13.42	75.7	14.51
S2 (15–45)	6.0	4.4	6.60	76.7	21.63
S3 (0–7)	5.8	4.2	117.72	27.3	66.63
S3 (7–27)	4.3	3.0	31.73	37.3	61.87
S4 (0–20)	4.9	4.1	31.91	35.2	40.99
Sodium aluminosilicate sorbent	5.96				

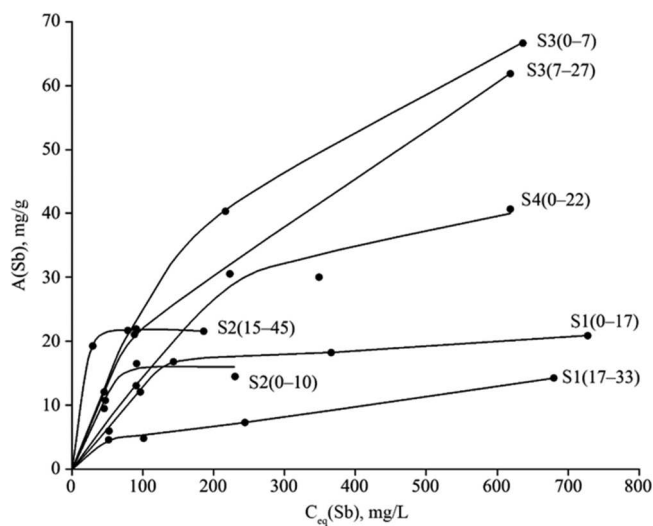


Figure 4. Sorption isotherms of Sb(III) ions by soils (numbering according to Table 1) under static conditions.

determined through thermal analysis. The derivatogram in Figure 5 indicates a minimum on the DTG curve between 180 and 350 °C and an exothermic effect with a maximum at 320 °C, which corresponds to the presence of polysaccharides such as cellulose and its derivatives [30]. The subsequent mass decrease and exothermic effect on the DSC curve are attributed to the oxidation of the carbonised residue.

The S3(0-7) sample was chosen for further study, because this soil type is more vulnerable to contamination by antimony compounds, but it can also serve as a sorption barrier to prevent antimony ions from entering the hydrological system, and has the most promising prospects for practical application. Additionally, the low degree of soil base saturation indicates minimal agricultural value.

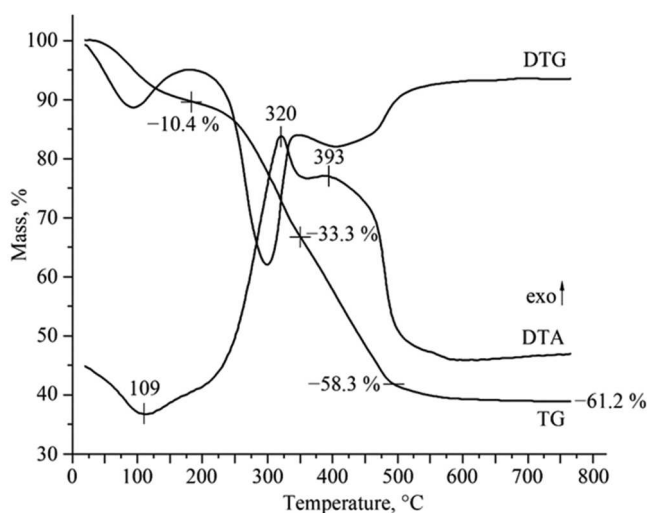


Figure 5. The thermogram of the soil S3(0-7) (numbering according to Table 2).

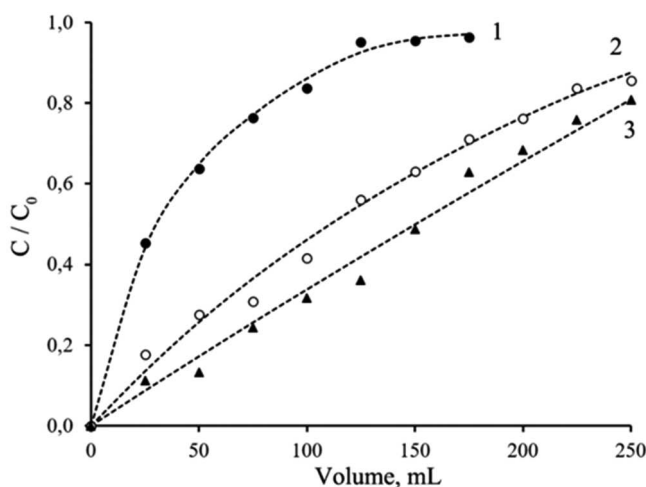


Figure 6. Output curves of antimony(III) ions sorption under dynamic conditions: 1 – soil S3(0–17); 2 – soil: sorbent = 1: 0.4; 3 – soil: sorbent = 1: 0.7

Table 4. Interphase distribution of antimony in the soil-sorbent system.

System, mass ratio	K_d (soil: sorbent)	K_d (solid: liquid)	Sb(III) extraction rate, %
Soil S3(0–17)	–	$2.12 \cdot 10^2$	8.21
Soil: sorbent 1: 0.4	1: 7.6	$4.63 \cdot 10^2$	41.04
Soil: sorbent 1: 0.7	1: 9.6	$7.02 \cdot 10^2$	53.00

To investigate the potential of using sorption barriers to protect soil from antimony contamination, the column experiment with layers of soil and aluminosilicate sorbent was performed. The barrier properties of the soil and a model combined system of a soil layer and a protective layer of sodium aluminosilicate sorbent were determined by output curves at different weight ratios of soil and sorbent (see Figure 6). The results show that the soil itself has barrier qualities. However, the practical use of a sorbent layer can increase the degree of groundwater purification and reduce the toxicological load on soils. Table 4 shows that using sodium aluminosilicate as a sorbent barrier increases the coefficient of interfacial distribution of antimony by 3.3 times and its extraction by 6.5 times.

Conclusion

Rice production waste, particularly rice straw, has been identified as a promising renewable raw material for the preparation of diverse sorption silicate materials. The sodium aluminosilicate synthesised from rice straw demonstrated a high sorption capacity for antimony(III) in both static and dynamic conditions. This indicates the potential for the use of this sorbent with capacity up to 113.9 g/kg in the form of sorption barriers to prevent the contamination of soils with antimony. The interaction of dissolved antimony with different soil types varies. This is the first study to demonstrate the dependence of the sorption characteristics of soil in relation to antimony on its composition and acid-

base parameters. The highest capacity values are observed at the maximum hydrolytic acidity and the minimum degree of soil base saturation. The sorption capacity of different types of soils for antimony is influenced by a combination of factors. In addition to the organic component content, cation exchange properties also play a role. From an ecological perspective, soils with high organic content and low base saturation are most susceptible to antimony contamination. Thus, data on the composition and properties of soils can serve as a basis for planning environmental protection measures, particularly the organisation of sorption barriers. Further development of this work will be directed toward the methods of remediation of already contaminated soils.

Acknowledgments

The collection of soil samples and determination of their physicochemical parameters were performed within the state assignment of the Ministry of Science and Higher Education of the Russian Federation FSC Biodiversity FEB RAS (topic No. 124012400285-7). The sorption properties were investigated, and aluminosilicate was synthesised and characterised as part of the State Assignment of the Institute of Chemistry, FEB RAS (FWFN(0205)-2022-0002). Atomic absorption analysis and energy-dispersive X-ray fluorescence spectroscopy were performed using equipment at the Far Eastern Centre for Structural Research, Institute of Chemistry, Far Eastern Branch, Russian Academy of Sciences.

Disclosure statement

No potential conflict of interest was reported by the author(s).

Data availability

Data will be made available on request.

Notes on contributors

A. N. Kholomeydik – Ph.D., research scientist of laboratory of Rare Metals Chemistry, Institute of Chemistry, Far-Eastern Branch, Russian Academy of Sciences.

A. E. Panasenko – Ph.D., chief of laboratory of Rare Metals Chemistry, Institute of Chemistry, Far-Eastern Branch, Russian Academy of Sciences.

I. V. Kiseleva – Ph.D., research scientist of laboratory of Soil Ecology, Federal Scientific Center of the East Asia Terrestrial Biodiversity, Far-Eastern Branch, Russian Academy of Sciences.

ORCID

A. N. Kholomeydik  <http://orcid.org/0000-0001-8280-6654>

A. E. Panasenko  <http://orcid.org/0000-0001-7875-6068>

I.V. Kiseleva  <http://orcid.org/0000-0002-2547-5905>

References

- [1] Zemnukhova LA, Davidovich RL, Udovenko AA et al. **Фторидные** комплексные соединения сурьмы (III). Синтез, строение, свойства, применение [Fluoride complexes of antimony(III). Synthesis, structure, properties and application]. Vladivostok; Ammonit; 2023. Russian.

- [2] Bartzas G, Komnitsas K. Solid phase studies and geochemical modelling of low-cost permeable reactive barriers. *J Hazard Mater.* **2010**;183(1–3):301–308. doi:[10.1016/j.jhazmat.2010.07.024](https://doi.org/10.1016/j.jhazmat.2010.07.024)
- [3] Wen B, Zhou J, Tang P, et al. Antimony (Sb) isotopic signature in water systems from the world's largest Sb mine, central China: novel insights to trace Sb source and mobilization. *J Hazard Mater.* **2023**;446:130622. doi:[10.1016/j.jhazmat.2022.130622](https://doi.org/10.1016/j.jhazmat.2022.130622)
- [4] Ahmad M, Lee SS, Moon DH, et al. A review of environmental contamination and remediation strategies for heavy metals at shooting range soils. In *Environmental Protection Strategies For Sustainable Development*. 2012. doi:[10.1007/978-94-007-1591-2_14](https://doi.org/10.1007/978-94-007-1591-2_14)
- [5] Liu J, Ding T, Fu S, et al. Genesis of the sanshiliuwan Sn-Pb-Zn-Sb deposit in the Xianghualing ore district (southern hunan, south China): constraints from geology, fluid inclusion analyses, and geochronology. *Ore Geol Rev.* **2023**;152:105227. doi:[10.1016/j.oregeorev.2022.105227](https://doi.org/10.1016/j.oregeorev.2022.105227)
- [6] Wu F, Fu Z, Liu B, et al. Health risk associated with dietary co-exposure to high levels of antimony and arsenic in the world's largest antimony mine area. *Sci Total Environ.* **2011**;409:3344–3351. doi:[10.1016/j.scitotenv.2011.05.033](https://doi.org/10.1016/j.scitotenv.2011.05.033)
- [7] Tokay B, Akpınar IA. Comparative study of heavy metals removal using agricultural waste bio-sorbents. *Bioresource Technology Reports.* **2021**;15:100719. doi:[10.1016/j.biteb.2021.100719](https://doi.org/10.1016/j.biteb.2021.100719)
- [8] Arthi D, Jose JMA, Gladis EHE, et al. Removal of heavy metal ions from water using adsorbents from agro waste materials. *Mater Today Proc.* **2021**;45:1794–1798. doi:[10.1016/j.matpr.2020.08.738](https://doi.org/10.1016/j.matpr.2020.08.738)
- [9] Naik RL, Kumar MR, Narsaiah TB. Removal of heavy metals (Cu & Ni) from wastewater using rice husk and orange peel as adsorbents. *Mater Today Proc.* **2023**;72:92–98. doi:[10.1016/j.matpr.2022.06.112](https://doi.org/10.1016/j.matpr.2022.06.112)
- [10] Qu Z, Leng R, Wang S, et al. Nanomaterials derived from metal–organic frameworks and their applications for pollutants removal. Review. *Reviews env. Contamination.* **2024**;262:12. doi:[10.1007/s44169-024-00064-2](https://doi.org/10.1007/s44169-024-00064-2)
- [11] Xie Y, Rong Q, Wen C, et al. Covalent organic framework with predesigned single-ion traps for highly efficient palladium recovery from wastes. *CCS Chemistry.* **2024**;6:1908–1919. doi:[10.31635/ccschem.023.202303404](https://doi.org/10.31635/ccschem.023.202303404)
- [12] Yuan L, Wang K, Zhao Q, et al. An overview of in situ remediation for groundwater co-contaminated with heavy metals and petroleum hydrocarbons. *J Environ Manag.* **2024**; 349. doi:[10.1016/j.jenvman.2023.119342](https://doi.org/10.1016/j.jenvman.2023.119342)
- [13] Scherer MM, Richter S, Valentine RL, et al. Chemistry and microbiology of permeable reactive barriers for in situ groundwater clean up. *Crit Rev Microbiol.* **2000**;26(4):221–264. doi:[10.1080/10408410091154237](https://doi.org/10.1080/10408410091154237)
- [14] Powell RM, Puls RW. Proton generation by dissolution of intrinsic or augmented aluminosilicate minerals for in situ contaminant remediation by zero-valence- state iron. *Environ Sci Technol.* **1997**;31(8):2244–2251. doi:[10.1021/es9607345](https://doi.org/10.1021/es9607345)
- [15] Antia DDJ. Hydrodynamic decontamination of groundwater and soils using ZVI. *Water (Basel).* **2023**; 15(3). doi:[10.3390/w15030540](https://doi.org/10.3390/w15030540)
- [16] Jayawardane WTH, Dayanthi WKC. Waste-derived permeable reactive barrier to treat heavy metals and organic matter in groundwater affected by landfill leachate. *Environmental Earth Sciences.* **2024**; 83(8). doi:[10.1007/s12665-024-11516-2](https://doi.org/10.1007/s12665-024-11516-2)
- [17] Zhang L, Lin Q, Guo X, et al. Sorption behavior of Florisil for the removal of antimony ions from aqueous solutions. *Water Sci Technol.* **2011**;63(10):2114–2122. doi:[10.2166/wst.2011.297](https://doi.org/10.2166/wst.2011.297)
- [18] Ilgen AG, Trainor TP. Sb(III) and Sb(V) sorption onto al-rich phases: hydrous al oxide and the clay minerals kaolinite KGa-1b and oxidized and reduced nontronite NAu-1. *Environ Sci Technol.* **2012**;46(2):843–851. doi:[10.1021/es203027v](https://doi.org/10.1021/es203027v)
- [19] Zhang X, Xie N, Guo Y, et al. Insights into adsorptive removal of antimony contaminants: functional materials, evaluation and prospective. *J Hazard Mater.* **2021**;418:126345. doi:[10.1016/j.jhazmat.2021.126345](https://doi.org/10.1016/j.jhazmat.2021.126345)
- [20] Dayanthi WKC, Jagoda SW, Hasini KAA. Laboratory experiments on remediation of landfill leachate contamination with permeable reactive barriers (PRBs) of reactive media derived from waste. *Engineer. J Inst Eng, Sri Lanka.* **2024**; 57(1). doi:[10.4038/engineer.v57i1.7640](https://doi.org/10.4038/engineer.v57i1.7640)
- [21] Kholomeidik AN, Panasenka AE. Recovery of Sb³⁺ ions by biogenic silicon-containing materials. *Russ J Inorg Chem.* **2022**;67:1465–1470. doi:[10.1134/s0036023622090066](https://doi.org/10.1134/s0036023622090066)

- [22] Isayev BN, Pavlik GN, Tsapkova NN, et al. Geochemical barriers as an effective method for geological environment protection. In: Colorado State University, editor. Tailings and mine waste '96. 1st ed. London: CRC Press; 2022. p. 291–293. doi:[10.1201/9781003077855-33](https://doi.org/10.1201/9781003077855-33)
- [23] Costa L, Martinez M, Suleiman M, et al. Manganese reductive dissolution coupled to Sb mobilization in contaminated shooting range soil. *Appl Microbiol Biotechnol.* 2024;108(1):295. doi:[10.1007/s00253-024-13133-2](https://doi.org/10.1007/s00253-024-13133-2)
- [24] IUSS Working Group WRB. World reference base for soil resources. In: Schad P, Mantel S, editors. International soil classification system for naming soils and creating legends for soil maps. 4th ed. Vienna, Austria: International Union of Soil Sciences; 2022. 234 p.
- [25] Агрохимические методы исследования почв [Agrochemical methods of soil research]. Moscow, Russian: Nauka; 1975.
- [26] Panasenko AE, Borisova PD, Arefieva OD, et al. Кислотно-основные свойства аморфного диоксида кремния из соломы и Шелухи риса [Aluminosilicates from rice straw: Obtaining and sorption properties]. *Khimiya Rastitel'nogo Syr'ya.* 2019; 3:291–298. Russian. doi:[10.14258/jcprm.2019034278](https://doi.org/10.14258/jcprm.2019034278)
- [27] Dovgan SV, Arefieva OD, Makarenko NV, et al. Извлечение Sb(III) из водных растворов алюмосиликатами из отходов производства риса [Extraction of Sb(III) from aqueous solutions with aluminosilicates from rice production waste]. *ChemChemTech [Izv. Vyssh. Uchebn. Zaved. Khim. Khim. Tekhnol.]*. 2022; 67 (4): 53–63. Russian. doi:[10.6060/ivkkt.20246704.6935](https://doi.org/10.6060/ivkkt.20246704.6935)
- [28] Kiseleva IV, Kholomeidik AN, Shchapova LN, et al. Impact of antimony fluoride compounds on soil microflora and methods of their detoxification. *Microbiology.* 2022;91:796–800. doi:[10.1134/S0026261722601427](https://doi.org/10.1134/S0026261722601427)
- [29] Gorbunova NS, Gromovik AI, Cherepukhina IV, et al. Сорбционные процессы в почвах. Вопросы изучения и современное состояние проблемы [Sorption processes in soils. Issues of study and current state of the problem]. *Sorbtsionnye i chromatograficheskie process.* 2021; 21(2):265–275. Russian. doi:[10.17308/sorpchrom.2021.21/3360](https://doi.org/10.17308/sorpchrom.2021.21/3360)
- [30] Chen Z, Wang X, Xue B, et al. Rice husk-based hierarchical porous carbon for high performance supercapacitors: The structure-performance relationship. *Carbon N Y.* 2020;161:432–444. doi:[10.1016/j.carbon.2020.01.088](https://doi.org/10.1016/j.carbon.2020.01.088)